CHAPTER IX

The Formation of a New Phase—Nucleation and Crystal Growth

1. Introduction

The transition from one phase to another is an important and interesting phenomenon closely linked to surface physical chemistry. The topic covers a wide range of situations from the ubiquitous process of rain formation in clouds to the formation of opals from monodisperse colloidal silica sediments. Quantitative description of nucleation and growth is challenging and has been attempted for many years in many contexts, such as the condensation of a vapor, the crystallization of a liquid and the precipitation of a solute from solution. The general formulation of the model for nucleation relies on application of bulk material properties to small clusters or droplets of material. Newer simulations and statistical mechanical density functional models improve on this assumption, but are not yet widely applicable and do not provide extensive improvements in the qualitative understanding of the process. In this chapter we focus on the nucleation and growth of solid materials, yet we formulate the general model for vapor–liquid nucleations as well.

In the absence of participating foreign surfaces, small clusters of molecules form and grow by accretion to the point of becoming recognizable droplets or crystallites that may finally coalesce or grow to yield large amounts of the new phase. This sequence generally does not occur if the system is just beyond the saturation pressure, concentration, or crystallization temperature. Instead, the concentration or vapor pressure must be increased well beyond the equilibrium value before nucleation in the form of a fog or suspension occurs. Similarly, pure liquids must be considerably supercooled prior to crystallization. Very pure liquid water can be cooled to −40°C before spontaneous freezing occurs; early observations of supercooling were made by Fahrenheit in 1714 [1].

The resistance to nucleation is associated with the surface energy of forming small clusters. Once beyond a critical size, the growth proceeds with the considerable driving force due to the supersaturation or subcooling. It is the definition of this *critical nucleus size* that has consumed much theoretical and experimental research. We present a brief description of the classic nucleation theory along with some examples of crystal nucleation and growth studies.

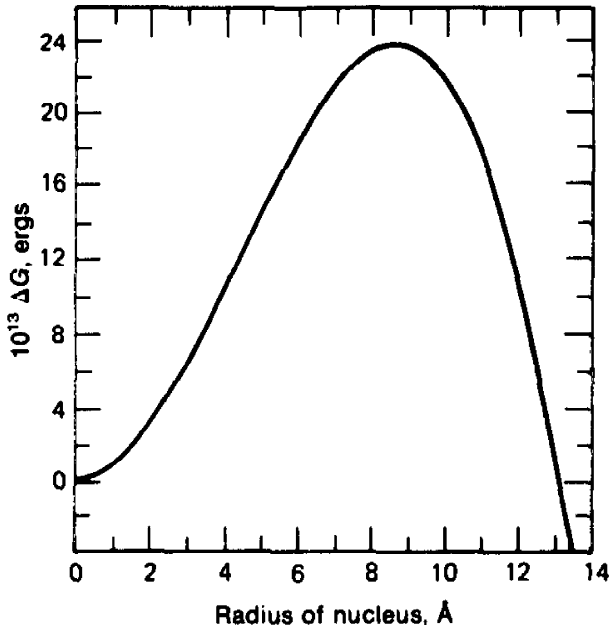

Fig. IX-1. Variation of ΔG with droplet size for water vapor at 0°C at four times the saturation pressure. (From Ref. 2.)

2. Classic Nucleation Theory

In the classic nucleation theory, the free energy of forming a cluster of radius r containing n atoms or molecules is the sum of two terms:

$$\Delta G = -n\,\Delta\mu + 4\pi r^2\gamma \tag{IX-1}$$

the driving force for the phase transition, $n\Delta\mu$, or energy to transfer n molecules from the one phase to another and the surface energy $4\pi r^2\gamma$ where γ is the interfacial tension. Since these terms are opposite in sign beyond the phase boundary, a plot of ΔG versus r goes through a maximum as illustrated in Fig. IX-1. For a condensation process at pressure P, $nA(\text{gas}) = A_n(\text{liq})$ the driving force becomes

$$\Delta G_{\text{cond}} = -n\Delta\mu = -nkT\ln\frac{P}{P^0} = -nkT\ln x \tag{IX-2}$$

where P^0 is the pressure or activity of the liquid phase. The number of molecules in the cluster is related to its size

$$n = \frac{4\pi}{3}\,r^3\hat{\rho} \tag{IX-3}$$

through the number density of the cluster, $\hat{\rho} = \rho N_A/M$ molecules/volume, where N_A is Avagadro's number and M is molecular weight. Combining Eqs. IX-1

and IX-3 and taking the derivative of the free energy with respect to radius or number and setting it equal to zero provides the value of n or r at the maximum, we obtain

$$n_c = \frac{32\pi\gamma^3}{3\hat{\rho}^2\,\Delta\mu^3} \tag{IX-4}$$

and

$$r_c = \frac{2\gamma}{\hat{\rho}\,\Delta\mu} \tag{IX-5}$$

defining the size of the critical nucleus. In the example presented in Fig. IX-1, the critical nucleus is about 8 Å in radius and contains about 90 molecules of water. For a liquid–vapor system, $r_c = 2\gamma/\hat{\rho}kT \ln x$ an equivalent of the Kelvin equation (Eq. III-21), giving the vapor pressure for a drop of radius r_c.

Combining Eqs. IX-1 and IX-5 gives the height of the energy barrier

$$\Delta G_{\max} = \frac{16\pi\gamma^3}{3\hat{\rho}^2\,\Delta\mu^2} = \frac{4\pi r_c^2\gamma}{3} \tag{IX-6}$$

which equals one-third of the surface energy for the formation of the nucleus as stated long ago by Gibbs [3]. When applied to crystals, Eq. IX-6 may have slight differences in the numerical factor since nonspherical shapes may be formed.

The dynamic picture of a vapor at a pressure near P^0 is then somewhat as follows. If P is less than P^0, then ΔG for a cluster increases steadily with size, and although in principle all sizes would exist, all but the smallest would be very rare, and their numbers would be subject to random fluctuations. Similarly, there will be fluctuations in the number of embryonic nuclei of size less than r_c, in the case of P greater than P^0. Once a nucleus reaches the critical dimension, however, a favorable fluctuation will cause it to grow indefinitely. The experimental maximum supersaturation pressure is such that a large traffic of nuclei moving past the critical size develops with the result that a fog of liquid droplets is produced.

It follows from the foregoing discussion that the essence of the problem is that of estimating the rate of formation of nuclei of critical size, and a semirigorous treatment has been given by Becker and Doring (see Refs. 4–6). The simplifying device that was employed, which made the treatment possible, was to consider the case of a steady-state situation such that the average number of nuclei consisting of 2, 3, 4, . . . , N molecules, although different in each case, did not change with time. A detailed balancing of evaporation and condensation rates was then set up for each size of nucleus, and by a clever integration procedure, the flux I, or the rate of formation of nuclei containing n molecules

from ones containing $n - 1$ molecules, was estimated. The detailed treatment is rather lengthy, although not difficult, and the reader is referred to Refs. 1, 2, and 4 through 7 for details.

The final equation obtained by Becker and Doring may be written down immediately by means of the following qualitative argument. Since the flux I is taken to be the same for any size nucleus, it follows that it is related to the rate of formation of a cluster of two molecules, that is, to Z, the gas kinetic collision frequency (collisions per cubic centimeter-second).

For the steady-state case, Z should also give the forward rate of formation or flux of critical nuclei, except that the positive free energy of their formation amounts to a free energy of activation. If one correspondingly modifies the rate Z by the term $e^{-\Delta G_{\max}/kT}$, an approximate value for I results:

$$I = Z \exp \frac{-\Delta G_{\max}}{kT} \tag{IX-7}$$

While Becker and Doring obtained a more complex function in place of Z, its numerical value is about equal to Z, and it turns out that the exponential term, which is the same, is the most important one. Thus the complete expression is

$$I = \frac{Z}{n_c} \left(\frac{\Delta G_{\max}}{3\pi kT} \right)^{1/2} \exp \frac{-\Delta G_{\max}}{kT} \tag{IX-8}$$

where n_c is the number of molecules in the critical nucleus. The quantity $(1/n_c)(\Delta G_{\max}/3\pi kT)^{1/2}$ has been called the *Zeldovich factor* [8, 9].

The full equation for I is obtained by substituting into Eq. IX-8 the expression for $\Delta G_{\max}$ and the gas kinetic expression for Z:

$$I = 2n^2\sigma^2 \left(\frac{RT}{M} \right)^{1/2} \exp \left[\frac{-16\pi\gamma^3 M^2}{3kT\rho^2 (RT \ln x)^2} \right] \tag{IX-9}$$

where σ is the collision cross section and n is the number of molecules of vapor per cubic centimeter. Since Z is roughly $10^{23}P^2$, where P is given in millimeters of mercury, Eq. IX-9 may be simplified as

$$I = 10^{23} P^2 \exp \frac{-17.5\overline{V}^2\gamma^3}{T^3(\ln x)^2} \text{ (in nuclei/cm}^3 \cdot \text{sec)} \tag{IX-10}$$

By way of illustration, the various terms in Eq. IX-10 are evaluated for water at 0°C in Table IX-1. Taking $\overline{V}$ as 20 cm^3/mole, γ as 72 ergs/cm^2, and P^0 as 4.6 mm, Eq. IX-10 becomes

TABLE IX-1
Evaluation of Equation IX-11 for Various Values of x

x	$\ln x$	$118/(\ln x)^2 = A$	e^{-A}	I, nuclei cm^{-3} sec^{-1}
1.0	0	—	0	0
1.1	0.095	1.31×10^4	10^{-5700}	10^{-5680}
1.5	0.405	720	10^{-310}	10^{-286}
2.0	0.69	246	10^{-107}	10^{-82}
3.0	1.1	95.5	10^{-42}	10^{-17}
3.5	1.25	75.5	10^{-33}	2×10^{-8}
4.0	1.39	61.5	$10^{-26.7}$	0.15
4.5	1.51	51.8	$10^{-22.5}$	10^3

$$I = 2 \times 10^{24} x^2 \exp\left[-\frac{118}{(\ln x)^2}\right] \tag{IX-11}$$

The figures in the table show clearly how rapidly I increases with x, and it is generally sufficient to define the critical supersaturation pressure such that $\ln I$ is some arbitrary value such as unity.

Frequently, vapor-phase supersaturation is studied not by varying the vapor pressure P directly but rather by cooling the vapor and thus changing P^0. If T_0 is the temperature at which the saturation pressure is equal to the actual pressure P, then at any temperature T, $P/P^0 = x$ is given by

$$\ln x = \frac{\Delta H_v}{R}\left(\frac{1}{T} - \frac{1}{T_0}\right) \tag{IX-12}$$

where ΔH_v is the latent heat of vaporization. Then, by Eq. IX-5, it follows that

$$\Delta T = T_0 - T = \frac{2\gamma M T_0}{r_c \Delta H_v \rho} = \frac{2\gamma \overline{V} T_0}{r_c \Delta H_v} \tag{IX-13}$$

[An interesting point is that ΔH_v itself varies with r [10].] As is the case when P is varied, the rate of nucleation increases so strongly with the degree of supercooling that a fairly sharp critical value exists for T. Analogous equations can be written for the supercooling of a melt, where the heat of fusion ΔH_f replaces ΔH_v.

At a sufficiently low temperature, the phase nucleated will be crystalline rather than liquid. The theory is reviewed in Refs. 1 and 7. It is similar to that for the nucleation

of liquid drops. The kinetics of the heterogeneous nucleation to form crystalline films on solid substrates has been simulated by means of Monte Carlo calculations [11, 12].

The case of nucleation from a condensed phase, usually that of a melt, may be treated similarly. The chief modification to Eq. IX-7 that ensues is in the frequency factor; instead of free collisions between vapor molecules, one now has a closely packed liquid phase. The rate of accretion of clusters is therefore related to the diffusion process, and the situation was treated by Turnbull and Fisher [13]. Again, the reader is referred to the original literature for the detailed derivation, and the final equation is justified here only in terms of a qualitative argument. If one considers a crystalline nucleus that has formed in a supercooled melt, then the rate at which an additional molecule may add can be regarded as determined by the frequency with which a molecule may jump from one position in the liquid to another just at the surface of the solid. Such a jump is akin to those involved in diffusion, and the frequency may be approximated by means of absolute rate theory as being equal to the frequency factor kT/h times an exponential factor containing the free energy of activation for diffusion. The total rate of such occurrences per cubic centimeter of liquid is

$$Z = n\,\frac{kT}{h}\exp\left(-\frac{\Delta G_D}{kT}\right) \tag{IX-14}$$

where n is the number of molecules of liquid per cubic centimeter. The steady-state treatment is again used, and the final result is analogous to Eq. IX-7:

$$I = n\,\frac{kT}{h}\exp\left(-\frac{\Delta G_D}{kT}\right)\exp\left(-\frac{\Delta G_{\max}}{kT}\right) \tag{IX-15}$$

For liquids that are reasonably fluid around their melting points, the kinetic factors in Eq. IX-15 come out about $10^{33}/\text{cm}^3 \cdot \text{sec}$, so that Eq. IX-15 becomes

$$I = 10^{33}\exp\left(-\frac{\Delta G_{\max}}{kT}\right) \tag{IX-16}$$

where $\Delta G_{\max}$ is given by Eq. IX-6, or by a minor modification of it, which allows for a nonspherical shape for the crystals.

A more recent model for the preexponential factor including viscous flow across the solid–liquid interface is [14]

$$Z = \frac{2(\gamma_{sl}kT)^{1/2}}{v_m^{5/3}\eta} \tag{IX-17}$$

where γ_{sl} is the interfacial energy per unit area of the solid–liquid interface, v_m is the molecule volume, and $\eta(T)$ is the liquid viscosity. Other preexponential factors have been proposed for solid-solid phase transitions [14].

Another important point in connection with the rate of nuclei formation in the case of melts or of solutions is that the rate reaches a maximum with degree of supercooling. To see how this comes about, r_c is eliminated between Eq. IX-6 and the one for liquids analogous to Eq. IX-13, giving

$$I = \frac{nkT}{h} e^{-A/kT} \tag{IX-18}$$

where

$$A = \Delta G_D + \frac{4\pi\gamma}{3} \left(\frac{2\overline{V}\gamma T_0}{\Delta H_f \Delta T} \right)^2$$

On setting dI/dT equal to zero, one obtains for y at the maximum rate the expression

$$\frac{(y-1)^3}{y^2(3-y)} = \frac{4\pi\gamma}{3\Delta H_D} \left(\frac{2\gamma\overline{V}}{\Delta H_f} \right)^2 \tag{IX-19}$$

where ΔH_D is the activation energy for diffusion, and $y = T_0/T$. Qualitatively, while the concentration of nuclei increases with increasing supercooling, their rate of formation decreases, due to the activation energy for diffusion or, essentially, due to the increasing viscosity of the medium. Glasses, then, result from a cooling so rapid that the temperature region of appreciably rapid nucleation is passed before much actual nucleation occurs (note Ref. 15).

Still another situation is that of a supersaturated or supercooled solution, and straightforward modifications can be made in the preceding equations. Thus in Eq. IX-2, x now denotes the ratio of the actual solute activity to that of the saturated solution. In the case of a nonelectrolyte, $x = S/S_0$, where S denotes the concentration. Equation IX-13 now contains ΔH_s, the molar heat of solution.

The classic nucleation theory is an excellent qualitative foundation for the understanding of nucleation. It is not, however, appropriate to treat small clusters as bulk materials and to ignore the sometimes significant and diffuse interface region. This was pointed out some years ago by Cahn and Hilliard [16] and is reflected in their model for interfacial tension (see Section III-2B).

Density functional theory from statistical mechanics is a means to describe the thermodynamics of the solid phase with information about the fluid [17–19]. In density functional theory, one makes an *ansatz* about the structure of the solid, usually describing the particle positions by Gaussian distributions around their lattice sites. The free

energy is then a functional of the local density in the lattice, which is approximated as a spatially varying *effective liquid*. Once this correspondence is made, the energy is easily integrated over the solid local density for the total free energy. The energy is minimized with respect to the Gaussian width to find the equilibrium structure and energy of the solid phase. Several averaging techniques have allowed its implementation to more complex problems of the interfacial tension between solids and liquids [20, 21]. Simple systems such as hard spheres [22], adhesive spheres [23, 24], and Lennard-Jones [21] molecules have been addressed; however, its widespread application to problems in crystal growth has been limited thus far.

The interfacial tension also depends on curvature (see Section III-1C) [25–27]. This alters Eq. IX-1 by adding a radius-dependent surface tension

$$\gamma(r) = \gamma^0 \left[1 - \frac{2\delta}{r} + O\left(\frac{1}{r^2}\right) \right] \tag{IX-20}$$

where now the Tolman length, δ can be expressed as $\delta = 2c_0K/\gamma^0$ in terms of the spontaneous curvature c_0 and the bending elastic modulus K and the second term is a complicated expression depending inversely on the square of the curvature. In practice, however, the first-order term may be negligible leaving only the $1/r^2$ dependence [27].

LaMer and Pound [28] noted that standard nucleation theory requires the use of the macroscopic interfacial tension down to critical nucleus sizes of about 1 nm. The exponential dependence on γ in Eq. IX-10 makes this a significant defect. An extreme case arises in condensation of mercury vapor because of the high liquid surface tension. The classical theory predicts a critical nucleus of only 1–10 *atoms* and underpredicts the critical supersaturation by a factor of 1000; a difference attributable to a 40% difference in the surface tension for the critical nuclei [29]. The surface tension may not vary strongly with size for more common materials. Benson and Shuttleworth [30] found that even for a crystallite containing 13 molecules the surface energy was only 15% less than that for a planar surface. Walton [31], with more allowance for distortion, found a 35% increase in the surface energy of a KCl crystal four ions in length. Condensation from a pure supersaturated gas, with no inert gas present, does not agree with theory perhaps due to a lack of a thermal steady state [32].

In principle, nucleation should occur for any supersaturation given enough time. The critical supersaturation ratio is often defined in terms of the condition needed to observe nucleation on a convenient time scale. As illustrated in Table IX-1, the nucleation rate changes so rapidly with degree of supersaturation that, fortunately, even a few powers of 10 error in the preexponential term make little difference. There has been some controversy surrounding the preexponential term and some detailed analyses are available [33–35].

Classic nucleation theory must be modified for nucleation near a critical point. Observed supercooling and superheating far exceeds that predicted by conventional theory and McGraw and Reiss [36] pointed out that if a usually neglected excluded volume term is retained the free energy of the critical nucleus increases considerably. As noted by Derjaguin [37], a similar problem occurs in the theory of cavitation. In binary systems the composition of the nuclei will differ from that of the bulk

vapor [38–40]; a controversy over this composition has been examined by Mirabel and Reiss [41].

3. Experimental Nucleation Studies

A. *One-Component Systems*

Many studies have been made on nucleation from a vapor, and generally the experimental findings are consistent with the Becker–Doring theory. Water has been a popular medium to study; Volmer and Flood [42] found the critical value of x to be about 5.03 for water vapor at 261 K while the theoretical value for $\ln I \approx 1$ is 5.14. Sander and Damköhler [43] found that the critical value of x for water and its temperature dependence were in reasonable agreement with theory. Some aspects of nucleation theory and experiments are reviewed by Higuchi and O'Konski [44] and some results are summarized in Table IX-2. In general, the agreement between theory and experiment is quite good as also supported by more recent work [45–48].

An important approach to the study of nucleation of solids is the investigation of small droplets of large molecular clusters. Years ago, Turnbull showed that by studying small droplets one could eliminate impurities in all except a few droplets and study homogeneous nucleation at significant undercoolings [13].

One remarkably simple yet seemingly robust outcome of Turnbull's experiments was his empirical finding that the solid–liquid interfacial free energy was

TABLE IX-2
Critical Supersaturation Pressures for Vapors

Substance	Temperature (K)	γ (erg/cm^2)	Critical value of x	
			Observed	Calculated
Water	275	—	4.2	4.2
	264	77.0	4.85	4.85
	261	—	5.0	5.1
Methanol	270	24.8	3.0, 3.2	1.8
Ethanol	273	24.0	2.3	2.3
n-Propanol	270	25.4	3.0	3.2
Isopropyl alcohol	265	23.1	2.8	2.9
n-Butyl alcohol	270	26.1	4.6	4.5
Nitromethane	252	40.6	6.0	6.2
Ethyl acetate	242	30.6	8.6–12	10.0
Dibutyl phthalate	332	29.4	26–29[a]	—
Triethylene glycol	324	42.8	27–37[a]	—

[a]Values of interfacial tension of nucleus from turbulent jet measurements, by various equations [44].

directly related to the enthalpy of fusion per molecule as [49]

$$\gamma_{sl} = C_T \, \Delta H_{\text{fus}} \hat{\rho}^{2/3} \tag{IX-21}$$

where C_T, the Turnbull coefficient, equals 0.45 for metals and 0.32 for other nonmetallic solids. This result has been confirmed for freezing of CCl_4 and $CHCl_3$ and has been extended to solid-solid transitions where ΔH for the transition is known and C_T = 0.2–0.3 [50]. It also agrees with density functional theory analysis (see Section IX-2A) of freezing in adhesive spheres where C_T = 0.47 for the entire phase diagram [23, 24].

Bartell and co-workers have made significant progress by combining electron diffraction studies from beams of molecular clusters with molecular dynamics simulations [14, 51, 52]. Due to their small volumes, deep supercoolings can be attained in cluster beams; however, the temperature is not easily controlled. The rapid nucleation that ensues can produce new phases not observed in the bulk [14]. Despite the concern about the appropriateness of the classic model for small clusters, its application appears to be valid in several cases [51].

The assumption that macroscopic interfacial tensions are valid down to critical nucleus size has led many researchers to use nucleation data to calculate interfacial tension. Staveley and co-workers [53, 54] used Eq. IX-16 to calculate the interfacial tensions for various organic and inorganic substances. Mason [55] estimated from the supercooling of water drops that the interfacial tension between ice and water was about 22 ergs/cm^2, in agreement with the 26 ergs/cm^2 from melting-point change in a capillary (Section X-2) and within range of Gurney's theoretical estimate of 10 ergs/cm^2 [56]. Turnbull and Cormia [57] give values of 7.2, 9.6, and 8.3 ergs/cm^2 for the solid–liquid interfacial tensions of *n*-heptadecane, *n*-octadecane, and *n*-tetracosane, respectively.

The entropically driven disorder–order transition in hard-sphere fluids was originally discovered in computer simulations [58, 59]. The development of colloidal suspensions behaving as hard spheres (i.e., having negligible Hamaker constants, see Section VI-3) provided the means to experimentally verify the transition. Experimental data on the nucleation of hard-sphere colloidal crystals [60] allows one to extract the hard-sphere solid–liquid interfacial tension, $\gamma = 0.55 \pm 0.02kT/\sigma^2$, where σ is the hard-sphere diameter [61]. This value agrees well with that found from density functional theory, $\gamma = 0.6 \pm 0.02kT/\sigma^2$ [21] (Section IX-2A).

An interesting experimental technique is "heat development" of nuclei. The liquid is held at the desired temperature for a prescribed time, while nuclei accumulate; they are then made visible as crystallites by quickly warming the solution to a temperature just below T_0, where no new nuclei form but existing ones grow rapidly.

Nucleation in a cloud chamber is an important experimental tool to understand nucleation processes. Such nucleation by ions can arise in atmospheric physics; theoretical analysis has been made [62, 63] and there are interesting differences in the nucleating ability of positive and negative ions [64]. In water vapor, it appears that the full heat of solvation of an ion is approached after only 5–10 water molecules have associated with

it. In a recent study using the common indoor pollutant radon to produce ions, He and Hopke [65] studied ion-induced particle formation that may have serious health effects if occurring in households.

B. Binary Systems and Solutions

As mentioned in Section IX-2A, binary systems are more complicated since the composition of the nuclei differ from that of the bulk. In the case of sulfuric acid and water vapor mixtures only some 10^{10} *molecules* of sulfuric acid are needed for water droplet nucleation that may occur at less than 100% relative humidity [38]. A rather different effect is that of "passivation" of water nuclei by long-chain alcohols [66] (which would inhibit condensation; note Section IV-6). A recent theoretical treatment by Bar-Ziv and Safran [67] of the effect of surface active monolayers, such as alcohols, on surface nucleation of ice shows the link between the inhibition of subcooling (enhanced nucleation) and the strength of the interaction between the monolayer and water.

The nucleation of a system by means of foreign bodies is, of course, a well-known phenomenon. Most chemists are acquainted with the practice of scratching the side of a beaker to induce crystallization. Of special interest, in connection with artificial rainmaking, is the nucleation of ice. Silver iodide, whose crystal structure is the same as ice and whose cell dimensions are very close to it, will nucleate water below −4°C [68]. Other agents have been found. A fluorophlogopite (a mica) does somewhat better than AgI [69] (see also Ref. 70). Fletcher [71] comments that the free energy barrier to the growth of an ice cluster on the surface of a foreign particle should be minimized if the particle-ice-water contact angle is small, which implies that the surface should be hydrophobic to water. A nucleating agent need not be crystalline. Thus ice nucleation can occur at a liquid interface [72].

A very different nucleation scheme by Grieser and co-workers employs ultrasonic irradiation of salt solutions to create H· and OH· radicals in solution [73]. These radicals proceed to nucleate growth of quantum-sized (Q-state) particles of cadmium sulfide. Similar initiation has been used for polymer latices [74].

Two nucleation processes important to many people (including some surface scientists!) occur in the formation of gallstones in human bile and kidney stones in urine. Cholesterol crystallization in bile causes the formation of gallstones. Cryotransmission microscopy (Chapter VIII) studies of human bile reveal vesicles, micelles, and potential early crystallites indicating that the cholesterol crystallization in bile is not cooperative and the true nucleation time may be much shorter than that found by standard clinical analysis by light microscopy [75]. Kidney stones often form from crystals of calcium oxalates in urine. Inhibitors can prevent nucleation and influence the solid phase and intercrystallite interactions [76, 77]. Citrate, for example, is an important physiological inhibitor to the formation of calcium renal stones. Electrokinetic studies (see Section V-6) have shown the effect of various inhibitors on the surface potential and colloidal stability of micrometer-sized dispersions of calcium oxalate crystals formed in synthetic urine [78, 79].

Supersaturation phenomena in solutions are, of course, very important, but, unfortu-

nately, data in this field tend to be not too reliable. Not only is it difficult to avoid accidental nucleation by impurities, but also solutions, as well as pure liquids, can exhibit memory effects whereby the attainable supersaturation depends on the past history, especially the thermal history, of the solution. In the case of slightly soluble salts, where precipitation is brought about by the mixing of reagents, it is difficult to know the effective degree of supersaturation.

If x is replaced by S/S_0, then Eq. IX-15 takes on the form

$$\ln t = k_1 - \frac{k_2\gamma^3}{T^3(\ln S/S_0)^2} \tag{IX-22}$$

and Stauff [80] found fair agreement with this equation in the case of potassium chlorate solutions. Gindt and Kern [81] took (N/t), the average rate of nucleation, as proportional to I, where N is the number of crystals produced, and from the slope of plots of log (N/t) versus $1/(\ln S/S_0)^2$ they deduced the rather low solid-solution interfacial tension value of 2–3 ergs/cm^2 for KCl and other alkali halides. Alternatively, one may make estimates from the critical supersaturation ratio, that is, the value of S/S_0 extrapolated to infinite rate of precipitation or zero induction time. Enüstün and Turkevich [82] found a value of 7.5 for $SrSO_4$, and from their solubility estimated interfacial tension (see Section X-2) deduced a critical nucleus of size of about 18 Å radius. More recently, Ring and co-workers gave nucleation rates of TiO_2 from alcohol solution [83, 84]. Uhler and Helz [85] studied the kinetics of PbS precipitating in the presence of a chelating agent.

4. Crystal Growth

The visible crystals that develop during a crystallization procedure are built up as a result of growth either on nuclei of the material itself or surfaces of foreign material serving the same purpose. Neglecting for the moment the matter of impurities, nucleation theory provides an explanation for certain qualitative observations in the case of solutions.

Once nuclei form in a supersaturated solution, they begin to grow by accretion and, as a result, the concentration of the remaining material drops. There is thus a competition for material between the processes of nucleation and of crystal growth. The more rapid the nucleation, the larger the number of nuclei formed before relief of the supersaturation occurs and the smaller the final crystal size. This, qualitatively, is the basis of what is known as von Weimarn's law [86]:

$$\frac{1}{d} = k\,\frac{S}{S_0} \tag{IX-23}$$

where d is some measure of the particle size. Although essentially empirical, the law appears to hold approximately.

A beautiful illustration of the balance between nucleation and crystal growth arises in the formation of "monodisperse" (i.e., narrow size distribution) colloids. One well-known example of such colloids occurs in natural opals formed from sediments of monodisperse silica particles [87]. Early work by LaMer and co-workers [88] showed that a short nucleation time followed by steady diffusion-limited growth produced monodisperse sulfur particles. More recent and broader studies by Matijevič and co-workers have encompassed a myriad of inorganic colloids [89–91]. This science involves the chemical processes resulting in an insoluble precipitate as well as the physical understanding of the particle nucleation and growth. An interesting feature of this work is that the final shape of the particles may not reflect the crystal structure (see Chapter VII) and may vary with experimental conditions. A good example of this occurs in ZnO (zincite) particles, all having the same crystal structure, prepared at different pH as shown in Figure IX-2.

The mechanism of crystal growth has been a topic of considerable interest. In the case of a perfect crystal, the starting of a new layer involves a kind of nucleation since the first few atoms added must occupy energy-rich positions. Becker and Doring [4],

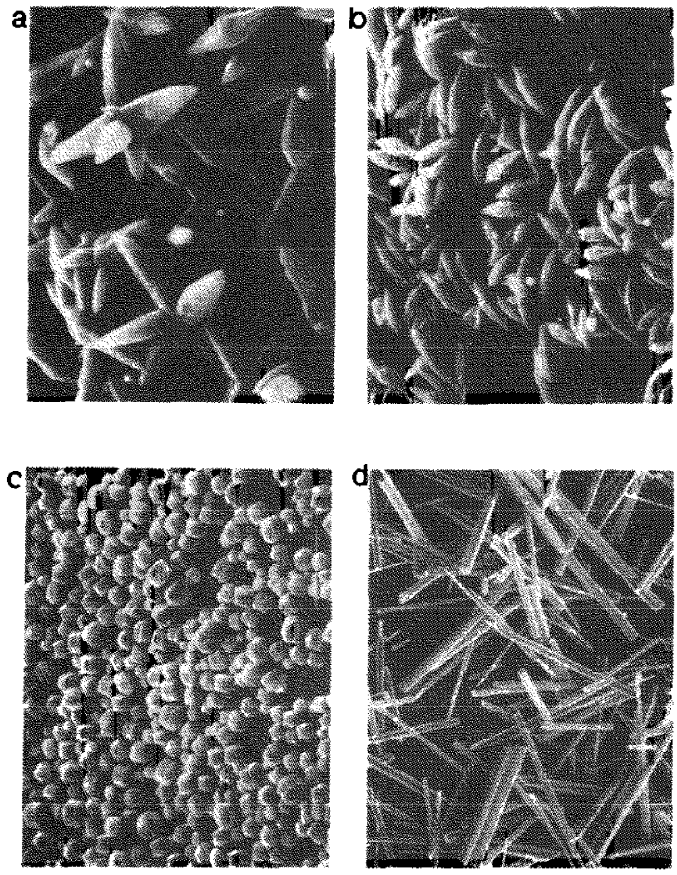

Fig. IX-2. SEM images of ZnO particles obtained by aging the following solutions: (*a*) $5.0 \times 10^{-3}M$ $Zn(NO_3)_2$ and $1.9 \times 10^{-2}M$ NH_4OH (pH 8.8) at 90°C for 3 hr; (*b*) $1.0 \times 10^{-4}M$ $Zn(NO_3)_2$ and $3.2 \times 10^{-4}M$ NH_4OH (pH 7.7) at 90°C for 1 hr; (*c*) $3.2 \times 10^{-3}M$ $Zn(NO_3)_2$ and 0.1 *M* triethanolamine (TEA, pH 8.9) at 90°C for 1 hr; (*d*) $4.0 \times 10^{-2}M$ $Zn(NO_3)_2$ and 0.2*M* TEA, and 1.2*M* NH_4OH (pH 12.1) at 150°C for 2 hr. The particles in (*a*), (*b*), and (*c*) average about 5 μm in size; those in (*d*) are much larger. (From Ref. 90.)

in fact, have treated crystal growth in terms of such surface nucleation processes; see also Ref. 60. Dislocations may also serve as surface nucleation sites, and, in particular, Frank [92] suggested that crystal growth might occur at the step of a screw dislocation (see Section VII-4C) so that the surface would advance in spiral form. However, while crystallization phenomena now occupy a rather large section of the literature, it is still by no means clear what mechanisms of crystal growth predominate. Buckley [93] comments that spiral patterns are somewhat uncommon and, moreover, occur on well-developed and hence *slowly* growing faces. Some interferometric studies of the concentration gradients around a growing crystal [94, 95] showed that, depending on the crystal, the maximum gradient may occur either near the center of a face or near the edges, and the pattern of fringes around a given crystal may change considerably from time to time and without necessarily any direct correlation with local growth rates. Clearly, the possibility of surface deposition at one point, followed by surface migration to a final site, must be considered. On the other hand, the Frank mechanism is widely accepted, and in individual cases it has been possible to observe the slow turning of a spiral pattern as crystal growth occurred [96]. The mechanism has been suggested in the case of some calcium phosphates [97].

The kinetics of crystal growth has been much studied; Refs. 98–102 are representative. Often there is a time lag before crystallization starts, whose parametric dependence may be indicative of the nucleation mechanism. The crystal growth that follows may be controlled by diffusion or by surface or solution chemistry (see also Section XVI-2C).

At equilibrium, crystal growth and dissolving rates become equal, and the process of *Ostwald ripening* may now appear, in which the larger crystals grow at the expense of the smaller ones. The kinetics of the process has been studied (see Ref. 103).

5. Epitaxial Growth and Surface Nucleation

The oriented overgrowth of a crystalline phase on the surface of a substrate that is also crystalline is called *epitaxial growth* [104]. Usually it is required that the lattices of the two crystalline phases match, and it can be a rather complicated process [105]. Some new applications enlist amorphous substrates or grow new phases on a surface with a rather poor lattice match.

In molecular beam epitaxy, evaporated atoms are directed toward a crystalline surface in an ultra-high-vacuum chamber, where in situ surface analysis may be performed (Chapter VIII). While epitaxial growth often requires lattice matching between the surface and the growing crystal phase, van der Waals interactions (see Chapter VI) dominate the growth of semiconductors and appear to relax the lattice matching constraint [106, 107]. Armstrong and co-workers have grown semiconductor GaSe and $MoSe_2$ films on GaP(111) after passivating the surface in a solution containing sulfur. The sulfur passivation creates a chemically unreactive smooth surface for the growth of semiconductor films. Molecular beam epitaxy of organic molecules creates ordered ultrathin films of large aromatic molecules on metals, insulators, and semiconductors [108] wherein the organic molecules are packed more closely than in films grown by Langmuir–Blodgett or self-assembly techniques (see Chapters XI and XV). Higher den-

sities may lead to improved optical properties in phthalocyanine dye thin films [109]. Again, van der Waals interactions seem to dominate the structures formed in organic films [110].

A very different type of epitaxial growth may be pursued in solutions. The desire to produce nanometer-sized semiconducting, metallic, or magnetic particles has fueled much recent research in surface chemistry. One name for this pursuit is "band-gap engineering." Fendler and co-workers have had success growing monodisperse crystals under Langmuir monolayers [111]. Infusing H_2S through a monolayer nucleates PbS crystals in a lead nitrate solution (see Figure VIII-3). With the appropriate choice of amphiphile, equilateral triangular crystallites of PbS can be grown with certain faces [such as (111)] oriented parallel to the monolayer [112]. Similar results are obtained with cadmium sulfide [113] and other semiconductors [111]. Electrocrystallization under monolayers is another means to control nanocrystal formation such as in the case of silver crystallization under various surfactants [114].

6. Problems

1. Calculate the value of the Zeldovich factor for water at 20°C if the vapor is 5% supersaturated.

2. Because of the large surface tension of liquid mercury, extremely large supersaturation ratios are needed for nucleation to occur at a measurable rate. Calculate r_c and n_c at 400 K assuming that the critical supersaturation is $x = 40{,}000$. Take the surface tension of mercury to be 486.5 ergs/cm^2.

3. Calculate ΔG of Eqs. IX-1 and IX-2 for the case of n-octane and plot against r over the range $r = 5$ to 300 Å and for the two cases of $x = 2$ and $x = 250$. Assume 20°C.

4. Assuming that for water ΔG_D is 7 kcal/mol, calculate the rate of nucleation for ice nuclei for several temperatures and locate the temperature of maximum rate. Discuss in terms of this result why glassy water might be difficult to obtain.

5. Calculate what the critical supersaturation ratio should be for water if the frequency factor in Eq. IX-10 were indeed too low by a factor of 10^{20}. Alternatively, taking the observed value of the critical supersaturation ratio as 4.2, what value for the surface tension of water would the "corrected" theory give?

6. Verify Fig. IX-1.

7. Given the expression IX-20 for the interfacial tension dependence on radius, derive the form of the dependence of the critical radius on the radius, given that the tension is proportional to (a) $1/r$ and (b) $1/r^2$.

8. Using the temperature dependence of γ from Eq. III-11 with $n = \frac{11}{9}$ and the chemical potential difference $\Delta\mu$ from Eq. IX-2, sketch how you expect a curve like that in Fig. IX-1 to vary with temperature (assume ideal-gas behavior).

9. As a follow-up to Problem 2, the observed nucleation rate for mercury vapor at 400 K is 1000-fold less than predicted by Eq. IX-9. The effect may be attributed to a lowered surface tension of the critical nuclei involved. Calculate this surface tension.

General References

F. F. Abraham, *Homogeneous Nucleation Theory*, Academic, New York, 1974.

H. E. Buckley, *Crystal Growth*, Wiley, New York, 1951.

P. P. Ewald and H. Juretschke, *Structure and Properties of Solid Surfaces*. University of Chicago Press, Chicago, 1953.

N. H. Fletcher, *The Physics of Rainclouds*, Cambridge University Press, Cambridge, England, 1962.

W. E. Garner, *Chemistry of the Solid State*, Academic, New York, 1955.

J. M. McBride, *Science*, **256,** 814 (1993).

K. Nishioka and G. M. Pound, *Surface and Colloid Science*, E. Matijevic, ed., Wiley, New York, 1976.

A. C. Zettlemoyer, ed., *Nucleation*, Marcel Dekker, New York, 1969.

Textual References

1. W. J. Dunning, *Nucleation*, Marcel Dekker, New York, 1969.
2. R. S. Bradley, *Q. Rev.* (London), **5,** 315 (1951).
3. J. W. Gibbs, *Collected Works of J. W. Gibbs*, Longmans, Green, New York, 1931.
4. R. Becker and W. Doring, *Ann. Phys.*, **24,** 719 (1935).
5. See M. Volmer, *Kinetik der Phasenbildung*, Edwards Brothers, Ann Arbor, MI, 1945.
6. F. F. Abraham, *Homogeneous Nucleation Theory*, Chapter V, Academic, New York, 1974.
7. J. Frenkel, *Kinetic Theory of Liquids*, Clarendon Press, Oxford, 1946.
8. P. P. Wegener, *J. Phys. Chem.*, **91,** 2479 (1987).
9. P. P. Wegener, *Naturwissenschaften*, **74,** 111 (1987).
10. A. W. Adamson and M. Manes, *J. Chem. Ed.*, **61,** 590 (1984).
11. A. I. Michaels, G. M. Pound, and F. F. Abraham, *J. Appl. Phys.*, **45,** 9 (1974).
12. G. H. Gilmer, H. J. Leamy, and K. A. Jackson, *J. Crystal Growth*, **24/25,** 495 (1974).
13. D. Turnbull and J. C. Fisher, *J. Chem. Phys.*, **17,** 71 (1949).
14. L. S. Bartell, *J. Phys. Chem.*, **99,** 1080 (1995).
15. E. Ruckenstein and S. K. Ihm, *J. Chem. Soc., Faraday Trans. I*, **72,** 764 (1976).
16. J. W. Cahn and J. E. Hilliard, *J. Chem. Phys.*, **31,** 688 (1959).
17. D. W. Oxtoby, "Liquids, Freezing and the Glass Transition," in *Les Houches Session 51*, J. P. Hansen, D. Levesque, and J. Zinn-Justin, eds., Elsevier, New York, 1990.
18. J. F. Lutsko, *Phys. Rev. A*, **43,** 4124 (1991).
19. Y. Singh, *Phys. Rep.*, **207,** 351 (1991).
20. A. R. Denton and N. W. Ashcroft, *Phys. Rev. A*, **39,** 4701 (1989).
21. D. W. Marr and A. P. Gast, *Phys. Rev. E*, **47,** 1212 (1993).
22. W. A. Curtin, *Phys. Rev. B*, **39,** 6775 (1989).

23. D. W. Marr and A. P. Gast, *J. Chem. Phys.*, **99,** 2024 (1993).
24. D. W. M. Marr and A. P. Gast, *Phys. Rev. E*, **52,** 4058 (1995).
25. See I. W. Plesner, *J. Chem. Phys.*, **40,** 1510 (1964).
26. R. A. Oriani and B. E. Sundquist, *J. Chem. Phys.*, **38,** 2082 (1963).
27. W. K. Kegel, *J. Chem. Phys.*, **102,** 1094 (1995).
28. V. K. LaMer and G. M. Pound, *J. Chem. Phys.*, **17,** 1337 (1949).
29. J. Martens, H. Uchtmann, and F. Hensel, *J. Phys. Chem.*, **91,** 2489 (1987).
30. G. C. Benson and R. Shuttleworth, *J. Chem. Phys.*, **19,** 130 (1951).
31. A. G. Walton, *J. Chem. Phys.*, **36,** 3162 (1963).
32. B. Barschdorff, W. J. Dunning, P. P. Wegener, and B. J. C. Wu, *Nat. Phys. Sci.*, **240,** 166 (1972).
33. H. Reiss, in *Nucleation II*, A. C. Zettlemoyer, ed., Marcel Dekker, New York, 1976.
34. H. Reiss, *Adv. Colloid Interface Sci.*, **7,** 1 (1977).
35. G. Wilemski, *J. Chem. Phys.*, **88,** 5134 (1988).
36. R. McGraw and H. Reiss, *J. Stat. Phys.*, **20,** 385 (1979).
37. B. V. Derjaguin, *J. Colloid Interface Sci.*, **38,** 517 (1972).
38. A. Jaecker-Voirol and P. Mirabel, *J. Phys. Chem.*, **92,** 3518 (1988).
39. G. Wilemski, *J. Phys. Chem.*, **91,** 2492 (1987).
40. C. Flageollet-Daniel, J. P. Garnier, and P. Mirabel, *J. Chem. Phys.*, **78,** 2600 (1983).
41. P. Mirabel and H. Reiss, *Langmuir*, **3,** 228 (1987).
42. M. Volmer and H. Flood, *Z. Phys. Chem.*, **A170,** 273 (1934).
43. A. Sander and G. Damköhler, *Naturwissenschaften*, **31,** 460 (1943).
44. W. L. Higuchi and C. T. O'Konski, *J. Colloid Sci.*, **15,** 14 (1960).
45. M. A. Sharaf and R. A. Dobbins, *J. Chem. Phys.*, **77,** 1517 (1982).
46. P. P. Wegener and C. F. Lee, *J. Aerosol Sci.*, **14,** 29 (1983).
47. P. P. Wegener, *J. Phys. Chem.*, **91,** 2479 (1987).
48. J. P. Garner, Ph. Ehrhard, and Ph. Mirabel, *Atmos. Res.*, **21,** 41 (1987).
49. D. Turnbull, *J. Appl. Phys.*, **21,** 1022 (1950).
50. T. S. Dibble and L. S. Bartell, *J. Phys. Chem.*, **96,** 8603 (1992).
51. J. Huang and L. S. Bartell, *J. Phys. Chem.*, **99,** 3924 (1995).
52. L. S. Bartell and J. Chen, *J. Phys. Chem.*, **99,** 12444 (1995).
53. H. J. de Nordwall and L. A. K. Staveley, *J. Chem. Soc.*, **1954,** 224.
54. D. G. Thomas and L. A. K. Staveley, *J. Chem. Soc.*, **1952,** 4569.
55. B. J. Mason, *Proc. Roy. Soc.* (London), **A215,** 65 (1952).
56. R. Shuttleworth, *Proc. Phys. Soc.* (London), **63A,** 444 (1950).
57. D. Turnbull and R. L. Cormia, *J. Chem. Phys.*, **34,** 820 (1961).
58. W. G. Hoover and F. H. Ree, *J. Chem. Phys.*, **49,** 3609 (1968).
59. B. Alder, W. Hoover, and D. Young, *J. Chem. Phys.*, **49,** 3688 (1968).
60. J. K. G. Dhont, C. Smits, and H. N. W. Lekkerkerker, *J. Colloid Interface Sci.*, **152,** 386 (1992).
61. D. W. Marr and A. P. Gast, *Langmuir*, **10,** 1348 (1994).

62. A. W. Castleman, Jr., P. M. Holland, and R. G. Keese, *J. Chem. Phys.*, **68,** 1760 (1978).
63. A. I. Rusanov, *J. Colloid Interface Sci.*, **68,** 32 (1979).
64. H. Rabeony and P. Mirabel, *J. Phys. Chem.*, **91,** 1815 (1987).
65. F. He and P. K. Hopke, *J. Chem. Phys.*, **99,** 9972 (1993).
66. B. V. Derjaguin, Yu. S. Kurghin, S. P. Bakanov, and K. M. Merzhanov, *Langmuir*, **1,** 278 (1985).
67. R. Bar-Ziv and S. A. Safran, *Phys. Rev. E*, **49,** 4306 (1994).
68. B. Vonnegut, *J. Appl. Phys.*, **18,** 593 (1947).
69. J. H. Shen, K. Klier and A. C. Zettlemoyer, *J. Atmos. Sci.*, **34,** 957 (1977).
70. V. A. Garten and R. B. Head, *Nature*, **205,** 160 (1965).
71. N. H. Fletcher, private communication.
72. J. Rosinski, *J. Phys. Chem.*, **84,** 1829 (1980).
73. R. A. Hobson, P. Mulvaney, and F. Grieser, *J. Chem. Soc., Chem. Commun.*, **1994,** 823.
74. S. Biggs and F. Grieser, *Macromolecules*, **28,** 4877 (1995).
75. A. Kapluna, Y. Talmon, F. M. Konikoff, M. Rubin, A. Eitan, M. Tadmor, and D. Lichtenberg, *Fed. Eur. Biochem. Soc. Lett.*, **340,** 78 (1994).
76. J. Callejas-Fernández, R. Martínez-García, F. J. de las Nieves López, and R. Hidalgo-Alvarez, *Solid State Ionics*, **63–65,** 791 (1993).
77. C. L. Erwin and G. H. Nancollas, *J. Crystal Growth*, **53,** 215 (1981).
78. J. Callejas-Fernández, F. J. de las Nieves, R. Martínez-García, and R. Hidalgo-Alvarez, *Prog. Colloid Polym. Sci.*, **84,** 327 (1991).
79. J. Callejas, R. Martínez, F. J. de las Nieves, and R. Hidalgo-Alvarez, *J. Surf. Sci. Technol.*, **8,** 105 (1992).
80. J. Stauff, *Z. Phys. Chem.*, **A187,** 107, 119 (1940).
81. R. Gindt and R. Kern, *CR*, **256,** 4186 (1963).
82. B. V. Enüstün and J. Turkevich, *J. Am. Chem. Soc.*, **82,** 4502 (1960).
83. M. D. Lamey and T. A. Ring, *Chem. Eng. Science*, **41,** 1213 (1986).
84. J. H. Jean and T. A. Ring, *Langmuir*, **2,** 251 (1986).
85. A. D. Uhler and G. R. Helz, *J. Crystal Growth*, **66,** 401 (1984).
86. P. P. von Weimarn, *Chem. Rev.*, **2,** 217 (1925).
87. P. J. Daragh, A. J. Gaskin, and J. V. Sanders, *Sci. Am.*, **234,** 84 (1976).
88. V. K. LaMer and R. H. Dinegar, *J. Am. Chem. Soc.*, **72,** 4847 (1950).
89. E. Matijević, *Langmuir*, **10,** 8 (1994).
90. E. Matijević, *Chem. Mat.*, **5,** 412 (1993).
91. E. Matijević, *Langmuir*, **2,** 12 (1986).
92. F. C. Frank, *Discuss. Faraday Soc.*, **5,** 48 (1949).
93. H. E. Buckley, in *Structure and Properties of Solid Surfaces*, R. Gomer and C. S. Smith, eds., University of Chicago Press, Chicago, 1952, p. 271.
94. G. C. Krueger and C. W. Miller, *J. Chem. Phys.*, **21,** 2018 (1953).
95. S. P. Goldsztaub and R. Kern, *Acta Cryst.*, **6,** 842 (1953).

96. W. J. Dunning, private communication.
97. G. H. Nancollas, *J. Crystal Growth*, **42,** 185 (1977).
98. G. L. Gardner and G. H. Nancollas, *J. Phys. Chem.*, **87,** 4699 (1983).
99. Z. Amjad, P. G. Koutsoukos, and G. H. Nancollas, *J. Colloid Interface Sci.*, **101,** 250 (1984).
100. C. Chieng and G. H. Nancollas, *Desalination*, **42,** 209 (1982).
101. Lj. Maksimović, D. Babić, and N. Kallay, *J. Phys. Chem.*, **89,** 2405 (1985).
102. D. Shea and G. R. Helz, *J. Colloid Interface Sci.*, **116,** 373 (1987).
103. D. B. Dadyburjor and E. Ruckenstein, *J. Crystal Growth*, **40,** 279, 285 (1977).
104. G. S. Swei, J. B. Lando, S. E. Rickert, and K. A. Mauritz, *Encyclopedia of Polymer Science and Technology*, Vol. 6, 2nd ed., Wiley, New York, 1986.
105. J. Heughebaert, S. J. Zawacki, and G. H. Nancollas, *J. Crystal Growth*, **63,** 83 (1983).
106. C. Hammond, A. Back, M. Lawrence, K. W. Nebesny, P. A. Lee, R. Schlaf, and N. R. Armstrong, *J. Vac. Sci. Technol. A*, **13,** 1768 (1995).
107. R. Schlaf, D. Louder, O. Lang, C. Pettenkofer, W. Jaegermann, K. W. Nebesny, P. A. Lee, B. A. Parkinson, and N. R. Armstrong, *J. Vac. Sci. Technol. A*, **13,** 1761 (1995).
108. T. J. Schuerlein, A. Schmidt, P. A. Lee, K. W. Nebesny, B. A. Parkinson, and N. R. Armstrong, *Jpn. J. Appl. Phys.*, **34,** 3837 (1995).
109. A. Schmidt, L. K. Chau, A. Back, and N. R. Armstrong, "Epitaxial Phthalocyanine Ultrathin Films Grown by Organic Molecular Beam Epitaxy (OMBE)," in *Phthalocyanines*, Vol. 4, C. Leznof and A. P. B. Lever, eds., VCH Publications, 1996.
110. C. D. England, G. E. Collins, T. J. Schuerlein, and N. R. Armstrong, *Langmuir*, **10,** 2748 (1994).
111. J. H. Fendler and F. C. Meldrum, *Adv. Mat.*, **7,** 607 (1995).
112. J. Yang and J. H. Fendler, *J. Phys. Chem.*, **99,** 5505 (1995).
113. J. Yang, F. C. Meldrum, and J. H. Fendler, *J. Phys. Chem.*, **99,** 5500 (1995).
114. N. A. Kotov, N. E. D. Zaniquelli, F. C. Meldrum, and J. H. Fendler, *Langmuir*, **9,** 3710 (1993).